THE JOURNAL OF BIOLOGICAL CHEMISTRY
Vol. 277, No. 35, Issue of August 30, pp. 32353–32359, 2002
Printed in U.S.A.

Growth Inhibitory Factor Prevents Neurite Extension and the Death of Cortical Neurons Caused by High Oxygen Exposure through Hydroxyl Radical Scavenging*

Received for publication, November 27, 2001, and in revised form, May 1, 2002
Published, JBC Papers in Press, June 10, 2002, DOI 10.1074/jbc.M111263200

Yoko Uchida‡§, Fujiya Gomi¶, Toshiki Masumizu‖, and Yuri Miura**

*From the Departments of ‡Neuropathology, ¶Ultrastructure, and **Biochemistry and Isotopes, Tokyo Metropolitan Institute of Gerontology, 35-2 Sakaecho, Itabashiku, Tokyo 173-0015 and the ‖3ESR Application Laboratory, JEOL Ltd., 3-1-2 Musashino, Akishimashi, Tokyo 196-8558, Japan*

Growth inhibitory factor (GIF), a brain-specific member of the metallothionein family (MT-III), has been characterized as a inhibitory substance for neurotrophic factors in Alzheimer's disease brains. However, the function of GIF, other than the inhibition of neurotrophic factors, remains unknown. We demonstrate here that exogenous GIF prevents neurite extension of cortical neurons in the early period of differentiation and the death of differentiated neurons caused by high oxygen exposure. Down-regulation of GIF in cortical neurons with antisense S-oligonucleotides promoted neuronal death under high oxygen conditions. ESR spin-trapping studies demonstrated that GIF at 2–6 μM scavenged hydroxyl radicals generated by a Fenton-type reaction or the photolysis of hydrogen peroxide much more effectively than the same concentration of metallothionein I+II. GIF did not scavenge either superoxide produced by the xanthine/xanthine oxidase reaction or NO generated from 1-hydroxy-2-oxo-3-(*N*-methyl-3-aminopropyl)-3-methyl-1-triazene. Moreover, GIF at 40–80 μM inhibited tyrosine nitration by peroxynitrite as efficiently as metallothionein I+II at the same concentration. These results indicate that GIF prevents neurite extension of neurons in the early period of differentiation and supports the survival of differentiated neurons by scavenging hydroxyl radicals.

Growth inhibitory factor (GIF)[1] is a brain-specific member of the metallothionein family (MT-III). Immunohistochemistry and immunoblot analysis indicate that GIF is distributed abundantly in astrocytes of the normal human brain but is reduced in astrocytes in the lesioned areas of neurodegenerative diseases, such as Alzheimer's disease (AD), amyotrophic lateral sclerosis, Down's syndrome, and Creutzfeldt-Jakob disease (1–4). GIF was characterized as an inhibitory substance for survival and neurite formation of cerebral cortical neurons in the presence of neurotrophic factors in AD brains (1). However, the function of GIF, other than the inhibition of neurotrophic factors, remains unknown. In the absence of neurotrophic factors, GIF is not toxic to neurons, but rather maintains the survival of neurons in culture (5). Moreover, MT-III (GIF)-overexpressing mice have enhanced resistance to neuronal injury induced by kainic acid, whereas MT-III-deficient mice have enhanced sensitivity to kainic acid (6, 7). These findings suggest that GIF may play a role in the protection of neurons against toxic substances. Although neurodegenerative diseases and seizures involve different etiological processes, oxidative stress is implicated in the pathogenesis and/or progression or at least as a final common mediator of neuronal death in both of these diseases. This suggests the possibility that GIF may act as a free radical scavenger. To test this possibility, we examined whether GIF prevents neurite extension from undifferentiated neurons and/or the death of differentiated neurons caused by reactive oxygen species in culture, and whether GIF has scavenging activities for superoxide, hydroxyl radicals, NO, or peroxynitrite.

EXPERIMENTAL PROCEDURES

Materials—5,5-Dimethylpyrroline 1-oxide (DMPO), diethylenetriamine pentaacetic acid (DTPA), 1-hydroxy-2-oxo-3-(*N*-methyl-3-aminopropyl)-3-methyl-1-triazene (NOC-7), 1,2-dimyristoylamido-1,2-deoxyphosphatidylcholine, 2-(4-trimethylammoniophenyl)-4,4,5,5-tetramethylimidazoline-1-oxyl 3-oxide chloride (TMA-PTIO), and peroxynitrite were purchased from Dojindo Laboratory (Kumamoto, Japan). L-α-Phosphatidylcholine from egg yolk was obtained from Nakalai Tesque, Inc. (Kyoto, Japan). C-DCDHF-DA was purchased from Molecular Probes, Inc. (Eugene, OR). L-Tyrosine, 3-nitro-L-tyrosine, and 3-chrolo-L-tyrosine were obtained from Sigma.

GIF and MT Proteins—Human GIF was isolated from human brain as previously described (1). Purified human GIF contained 4 copper and 3 zinc atoms per polypeptide chain. Rat GIF was purified from rat brain according to the procedure reported previously (8). Average metal content in purified rat GIF was 2.22 copper and 0.09 zinc atoms per polypeptide chain (Cu-GIF), because of 0.02 N HCl (pH 2.5) treatment at the first step of purification. After the addition of zinc and copper to Cu-GIF, average metal content of GIF increased to 3.12 copper and 2.13 zinc atoms per polypeptide chain (Cu,Zn-GIF). The concentration of GIF protein in cell lysate or medium was measured by two-site ELISA as previously described (8). Rabbit liver metallothionein I+II (Cd,Zn-MT) was obtained from Sigma. GIF and MT-I+II were dissolved in 0.1 M phosphate-buffered saline (PBS) at pH 7.4.

Cell Culture—For neuronal cell culture, cerebral cortices dissected from embryonic day 17 rats were dissociated by incubation with 0.08%

* This work was supported by Grant-in-aid for Scientific Research (C) 08838033 from the Ministry of Education, Science and Culture, and by grants-in-aid from the Ministry of Health and Welfare. The costs of publication of this article were defrayed in part by the payment of page charges. This article must therefore be hereby marked "*advertisement*" in accordance with 18 U.S.C. Section 1734 solely to indicate this fact.

§ To whom correspondence should be addressed. Tel.: 813-3964-3241 (ext. 3050); Fax: 813-3579-4776.

[1] The abbreviations used are: GIF, growth inhibitory factor; AD, Alzheimer's disease; C-DCDHF-DA, 6-carboxy-2′,7′-dichlorodihydrofluorescein diacetate, di(acetoxymethyl ester); DMPO, 5,5′-dimethylpyrroline 1-oxide; MT-I+II, metallothionein I+II; MT-III, metallothionein III; ODN, oligodeoxynucleotide; ROS, reactive oxygen species; SOD, superoxide dismutase; MEM, minimal essential medium; ANOVA, analysis of variance; PTI, 2-phenyl-4,4,5,5-tetramethylimidazoline-1-oxyl; PTIO, 2-phenyl-4,4,5,5-tetramethylimidazoline-1-oxyl3-oxide; NOC-7, 1-hydroxy-2-oxo-3-(*N*-methyl-3-aminopropyl)-3-methyl-1-triazene; PI, propidium iodide; ELISA, enzyme-linked immunosorbent assay; mT, millitesla; PBS, phosphate-buffered saline; TMA-PTIO, 2-(4-trimethylammoniophenyl)-4,4,5,5-tetramethylimidazoline-1-oxyl 3-oxide chloride; DTPA, diethylenetriamine pentaacetic acid; DIV, days *in vitro*.

trypsin, 0.008% DNase I at 37 °C for 10 min, and passed through a 62-μm nylon mesh. To assess neuronal survival, cerebral cortical cells (1.85×10^4 cells/well) in 96-well microtiter plates coated with gelatin-polyornithine were cultured for 5 days in MEM plus 5% fetal bovine serum containing 10 μM β-mercaptoethanol under air plus 5% CO_2. Then the cells were incubated in MEM-N2-pyruvate medium with or without GIF under 50% O_2 + 5% CO_2 for an additional 48 h. Neuronal survival was assessed by quantifying anti-MAP2 binding to the cultured cells using ELISA (9). To assess neurite outgrowth, cerebral cortical cells (3×10^4 cells/well) seeded in multiwell plates (9 × 9 mm) precoated with gelatin-polyornithine, were cultured for 12 h in MEM plus 5% fetal bovine serum with or without GIF under 50% O_2 + 5% CO_2. Cell were fixed and labeled with β-tubulin monoclonal antibody (Amersham Biosciences) by the avidin-biotin peroxidase method. The neurite length was determined by measuring the distance between the end of the longest neurite and the cell surface. This measurement was done for 150 neurons in 18 or 19 fields in each experiment.

Astrocyte cultures were prepared from the cerebral cortex of postnatal day 2 rats and subcultured three times as previously described (8).

S-oligonucleotide Transfections—An antisense S-oligodeoxynucleotide (S-ODN) directed against bases 53–76 (initial codon at 62) of rat GIF mRNA (10) (GenBank™ accession number not available) (5′-GGTCTCAGGGTCCATATCCAGGCC-3′), a scrambled S-ODN (5′-CCGGCTGGTCTCAGGGTCCATATC-3′), and a sense GIF S-ODN (5′-GGCCTGGATATGGACCCTGAGACC-3′) were synthesized by Nippon Seifun. A fluorescein isothiocyanate-labeled antisense S-ODN at the 5′ end was also synthesized to monitor transfection efficiency to cortical neurons. Cultured cells were transfected with S-ODNs (250 nM) using OligofectAMINE (Invitrogen) twice at 15-h intervals. Thirty hours after the first transfection, cells were re-treated with S-ODNs alone in MEM-N2 pyruvate and maintained for an additional 24 h under 5% CO_2 plus air or 50% oxygen. Fifty-four hours after the first transfection, the cells were analyzed for GIF protein level by two-site ELISA (8) and for neuronal death by propidium iodide (PI) assay. Briefly, cells were incubated with PI (20 μM) and Hoechst 33342 (10 μM) solution (in PBS) for 10 min. After fixation, dead cell nuclei were visualized in red fluorescence with PI and nuclei of both live and dead cell were visualized with Hoechst 33342. The transfection efficiencies of antisense ODN as determined by fluorescein isothiocyanate fluorescence of targeted neurons were almost 100%.

Measurement of Intracellular ROS by Flow Cytometry—The lipophilic fluorogen C-DCDHF-DA is retained in viable cells and converted intracellularly to a fluorescent molecule by oxidization. The fluorescence intensity thus depends on the amount of intracellular peroxide. Cultured neurons were incubated with C-DCDHF-DA at a final concentration of 10 μM for 10 min at 37 °C under 5% CO_2 plus air. Cells were dissociated by pipetting, and the fluorescence intensity of the cells was analyzed using an EPICS ELITE cell sorter.

ESR Spectroscopy and Spin Trapping—Superoxide radical was generated from a hypoxanthine xanthine oxidase reaction under the conditions as previously reported (11). In the presence of the spin trap, DMPO, the superoxide was produced as the more stable spin adduct, DMPO-O_2^-. ESR spectra of DMPO-O_2^- were acquired using a JES-FA200 (JEOL), operating at an incident micropower of 8 milliwatts, a modulation amplitude of 0.1 mT, a time constant of 0.1 s, and sweep rate of 5 mT/min. Cu,Zn-SOD was used as a standard inhibitor of DMPO adduct production because the decrease in DMPO-O_2^- signal intensity correlated with the SOD concentration (11).

Hydroxyl radical, generated in a Fenton-type reaction between 0.34 mM H_2O_2 and 0.34 mM Fe^{2+} chelated with 0.34 mM DTPA in 0.1 M PBS (pH 7.4), was trapped with 83.6 mM DMPO to produce a stable hydroxyl radical spin adduct (DMPO-OH), which can be monitored by ESR spectroscopy. The signal intensities of DMPO-OH were evaluated by the relative peak height of DMPO-OH to the intensity of the Mn^{2+} signal. One hundred percent DMPO-OH represented the signal intensity of DMPO-OH obtained in the absence of the proteins. The concentration of GIF required to reduce the signal intensity of DMPO-OH by 50%, ID_{50}, was determined by using 83.6 mM DMPO and five concentrations of GIF (0.38, 0.77, 1.53, 3.06, and 6.12 μM). The bimolecular rate constant for the reactions of the hydroxyl radical with GIF was calculated by using the following expression: $k_{GIF/\cdot OH} = k_{DMPO/\cdot OH} \times [DMPO]/ID_{50}$ of GIF, according to the method of Mitsuta (11).

Nitric oxide, generated from NOC-7, was trapped with PTIO in liposomes to produce a stable PTI in liposome vesicles. Liposome PTIO was prepared by a reversed-phase evaporation method as described (12), by using L-α-phosphatidylcholine from egg yolk, 1,2-dimyristoylamido-1,2-deoxyphosphatidylcholine, and TMA-PTIO. The concentration of liposome PTIO was determined from the double integration of the ESR signal with TMA-PTIO as a standard. NOC-7 (10 μM) was added to the mixture of GIF solution and liposome PTIO (25 μM) suspension, and incubated for 15 min at 37 °C. PTI and unreacted PTIO were monitored by ESR spectroscopy, and the relative signal intensities of PTI were calculated according to the previous report (12).

Quantification of Peroxynitrite—Peroxynitrite (final concentration 1.22 mM) was added to the mixture of L-tyrosine (final concentration 1 mM) and proteins (GIF or MT-I+II) in 0.1 M PBS (pH 7.4) and incubated for 10 min at 37 °C. At the end of the incubation, 3-chloro-L-tyrosine (final concentration of 0.01 mM) was added to the reaction mixture as an internal standard. The 3-nitro-L-tyrosine produced in the reaction mixture was analyzed by VP-318 reverse phase high performance liquid chromatography according to the method of Nakagawa (13).

RESULTS

Secretion of GIF from Cultured Astrocytes—To examine whether GIF is secreted from astrocytes, we measured the amount of cellular GIF and extracellular GIF secreted from astrocytes (23 days *in vitro* (DIV)) into the medium over a 24-h period by using the two-site ELISA of rat GIF. The cellular content of GIF in astrocytes cultured in serum-free medium was 135.72 ± 42.48 (mean ± S.E.) ng/mg of protein ($n = 3$). The extracellular:intracellular ratio of GIF was 1.29 ± 0.40 ($n = 3$), whereas the extracellular:intracellular ratio of lactate dehydrogenase was 0.072 ± 0.003 ($n = 3$), indicating that extracellular GIF does not result from cell lysis in the culture. It is possible that GIF is stored and secreted by a regulated pathway (14).

Effects of Exogenous GIF on Neuronal Survival and Neurite Extension—To examine the effects of GIF on cortical neurons, other than inhibition of neurotrophic factors in AD brains, 0 or 5 DIV neurons were used for the assessment of GIF effects on neurite extension or neuronal survival, respectively. As shown in Fig. 1*A*, the addition of 100 nM GIF shifted the peak of neurite length to a shorter range. The average neurite lengths of control (2.53 ± 0.11 μm) and GIF-treated neurons (1.85 ± 0.09 μm) were significantly different ($p < 0.0001$). Fig. 1*B* shows that the addition of GIF at 125–250 nM did not inhibit but rather supported the survival of 5 DIV neurons cultured for an additional 2 days ($p < 0.01$). GIF at up to 1 μM did not inhibit but rather supported the survival of cortical neurons (data not shown). In contrast to GIF, Zn7-MT-I+II at 125 nM did not support neuronal survival. These results indicate that GIF suppresses the neurite extension from neurons in the early period of differentiation and suppresses cell death of more differentiated neurons.

Prevention of Neurite Extension and Neuronal Death under High Oxygen by GIF—Hyperoxia is stimulus for neuronal cells that may cause either differentiation (15) or cell death (16). Therefore, it is possible to speculate that the prevention of neuronal differentiation and death by GIF is mediated by a scavenging activity of GIF for reactive oxygen species (ROS). To test this hypothesis, we investigated whether GIF prevents neurite extension and neuronal death under a high oxygen atmosphere. As shown in Fig. 2*A*, exposure of cortical neurons to high oxygen shifted the peak of neurite length to a longer range; however, the addition of 100 nM GIF in the medium shifted the peak of neurite length back to a shorter range than that of the control cultures. The average neurite length of neurons exposed to high oxygen (2.66 ± 0.08 μm) and that of neurons treated with both GIF and high oxygen (1.98 ± 0.09 μm) were significantly different ($p < 0.0001$). Fig. 2*B* shows that high oxygen exposure reduced neuronal survival to 37.8 ± 2.4% in the absence of GIF. The addition of GIF (100 nM) but not of Zn7-MT-I+II (100 nM) partially prevented neuronal death by high oxygen ($p < 0.01$). The effect of GIF up to 300 nM on preventing neuronal death by high oxygen exposure was the same as that of 100 nM GIF (data not shown). These results suggest that GIF prevents neuronal differentiation and neuronal death induced by high oxygen exposure.

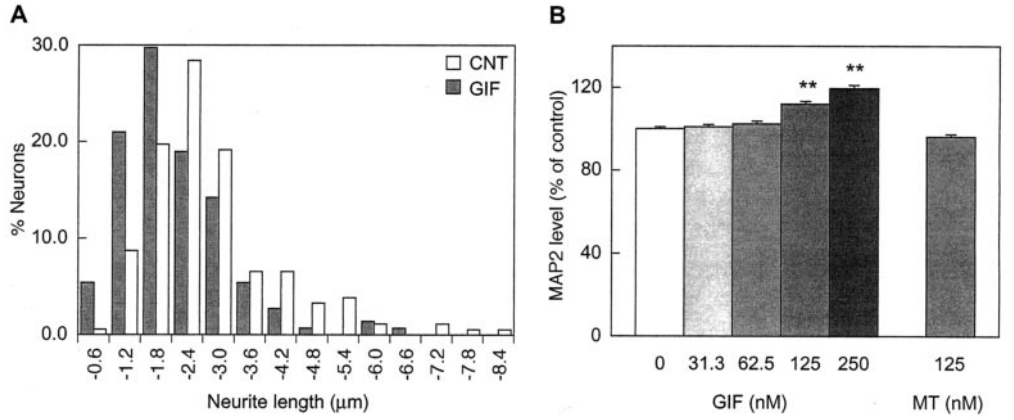

FIG. 1. **GIF inhibited the neurite extension from 0-days-*in vitro* (0 DIV) cortical neurons (*A*) but did not inhibit the survival of 5 DIV cortical neurons (*B*).** *A*, cortical neurons were seeded and cultured for 12 h with or without human GIF (final concentration 100 nM) under air plus 5% CO_2. Neurite length from each neuron was determined as indicated under "Experimental Procedures." The average neurite lengths of control (2.53 ± 0.11 μm, $n = 150$) and GIF-treated neurons (1.85 ± 0.09 μm, $n = 150$) were significantly different ($p < 0.0001$). *B*, five DIV neurons were incubated for an additional 48 h with various concentrations of human GIF under air plus 5% CO_2. The remaining neurons were assayed by ELISA for anti-MAP2 binding as indicated under "Experimental Procedures." Results are expressed as a percentage of the untreated control value. Data are mean ± S.E. of two independent experiments with five determinations each. **, $p < 0.01$ by ANOVA and the *post hoc* test compared with control.

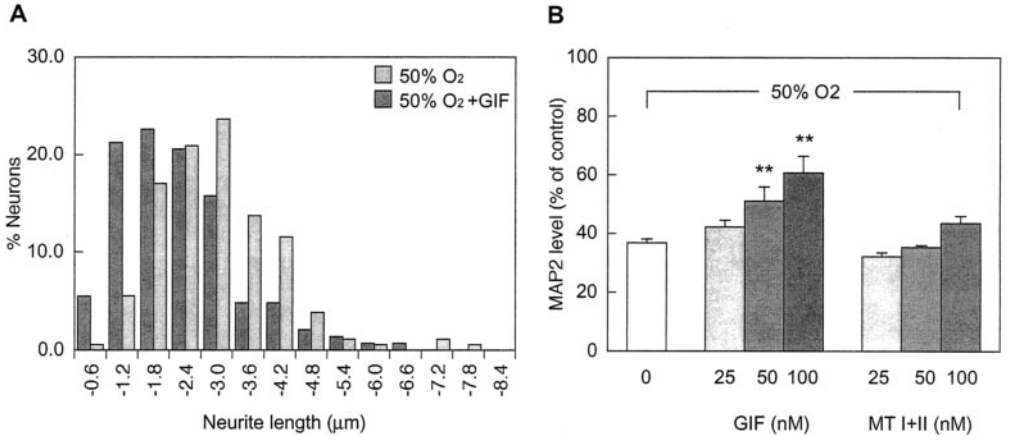

FIG. 2. **GIF prevented the neurite extension (*A*) and neuronal death (*B*) caused by high oxygen atmosphere.** *A*, cortical neurons were seeded and cultured for 12 h with or without human GIF (final concentration 100 nM) under 50% oxygen. Neurite length was determined as indicated under "Experimental Procedures." The average neurite lengths of neurons cultured without GIF (2.66 ± 0.08 μm) and those cultured with GIF (1.98 ± 0.09 μm) were significantly different ($p < 0.0001$). *B*, five DIV neurons were cultured for an additional 48 h with various concentrations of human GIF under 50% oxygen. Neuronal survival was assessed by ELISA for anti-MAP2 binding as indicated under "Experimental Procedures." Results are expressed as a percentage of the untreated control value. Data are mean ± S.E. of two independent experiments with five determinations each. **, $p < 0.01$ by ANOVA and the *post hoc* test compared with the culture without GIF under 50% oxygen.

Enhancement of Neuronal Vulnerability to High Oxygen by Antisense Oligodeoxynucleotides for GIF—To confirm the protective action of GIF against neuronal death by high oxygen exposure, we examined whether the down-regulation of GIF in cortical neurons by a GIF antisense ODN results in the promotion of neuronal death. GIF protein level in transfected astrocytes with antisense ODN (250 nM) for 56 h decreased by 4-fold compared with the level in transfected astrocytes with sense or scramble ODNs (Fig. 3*A*). The basal GIF level in cultured neurons was detectable but lower (~50 ng/mg of protein) than that in astrocytes. The GIF level in transfected neurons with antisense ODN was below the detection limit in the two-site ELISA (data not shown). As shown in Fig. 3*B*, the down-regulation of GIF in cortical neurons with antisense ODN promoted neuronal death by 2-fold under 50% oxygen atmosphere for 24 h. Transfection with scramble or sense ODNs did not promote neuronal death by high oxygen exposure for 24 h. These results indicate that down-regulation of GIF in cortical neurons promotes neuronal death induced by high oxygen exposure.

Reduction of Intracellular ROS Production by GIF—To examine whether exogenous GIF reduced the ROS production in cultured neurons, C-DCDHF-DA was added to the neurons cultured for 48 h under 50% O_2 + 5% CO_2. After additional incubation for 10 min at 37 °C under 5% CO_2 plus air, cells were dissociated by pipetting and the fluorescence intensity of the cells was analyzed by flow cytometry. Fig. 4 shows typical histograms of ROS production in cortical neurons exposed to 50% O_2 for 48 h in the absence or presence of 100 nM GIF in the medium. GIF effectively reduced the ROS production in cortical neurons under 50% oxygen atmosphere.

GIF Has Scavenging Activity for Hydroxyl Radicals and Peroxynitrite but Not for Superoxide or NO—We assessed the scavenging activity of GIF for superoxide, hydroxyl radicals, and NO by using ESR spin-trapping. The superoxide scavenging activities of human GIF or rabbit liver MT-I+II, evaluated using Cu,Zn-SOD as a standard, were 5.96 or 7.56 units of SOD equivalent/mg of protein, respectively. The activity of Cu,Zn-SOD used here was 3700 units/mg of protein, indicating that the scavenging activities of GIF or MT-I+II are very weak.

Fig. 5 (*A* and *B*) shows that the signal intensities of

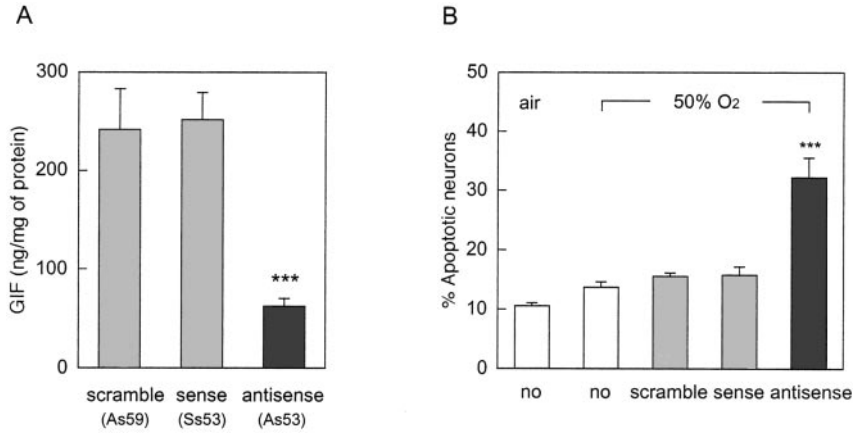

FIG. 3. **Antisense ODN for GIF decreased GIF protein level in cultured astrocytes (*A*) and accelerated neuronal death caused by high oxygen exposure (*B*).** Cortical neurons at 4 DIV were transfected with scramble, sense, or antisense ODNs (250 nM each) using OligofectAMINE (Invitrogen) twice at 15-h intervals. Thirty hours after the first transfection, cells were re-treated with S-ODNs alone in MEMN2 and maintained for an additional 24 h under 5% CO_2 plus air (*A*) or 50% oxygen (*B*). *A*, the GIF protein concentration in the astrocyte cultures 54 h after the first transfection was determined by the two-site ELISA for rat GIF. *B*, neuronal death of the cultures exposed to 50% oxygen was assessed by propidium iodide assay 54 h after the first transfection as indicated under "Experimental Procedures." Data are mean ± S.E. of two independent experiments with four determinations each. ***, $p < 0.0001$ by ANOVA and the *post hoc* test compared with cultures without ODN under 50% oxygen.

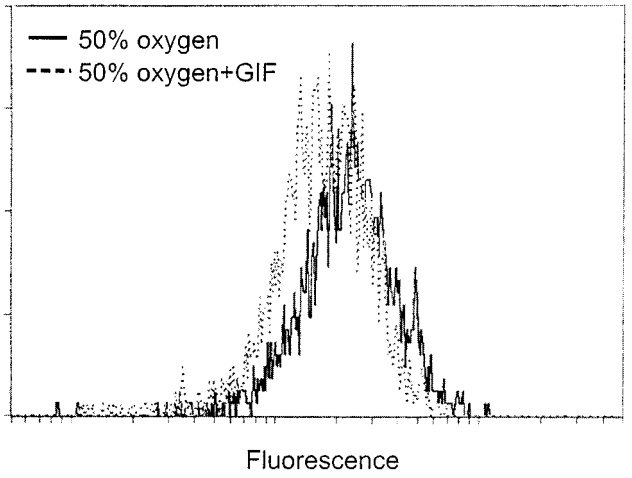

FIG. 4. **GIF decreased intracellular ROS production in cortical neurons cultured for 48 h under 50% oxygen atmosphere.** Cortical neurons at 5 DIV were cultured for 48 h under 50% oxygen in the presence or absence of 100 nM GIF. Neurons were then incubated with C-DCDHF-DA at final concentration of 10 μM for 10 min at 37 °C under 5% CO_2 plus air. Cells were dissociated by pipetting, and the fluorescence intensity of the cells was analyzed using an EPICS Elite cell sorter.

DMPO-OH markedly decreased in the presence of GIF, but not of MT-I+II, in a Fenton-type hydroxyl radical generating system. As shown in Fig. 5*C*, a dose-dependent decrease in the intensity of DMPO-OH was observed in the presence of GIF. To exclude possible effects caused by metal exchange between copper or zinc in GIF and Fe in the Fenton reaction, we used another hydroxyl radical generating system involving the photolysis of hydrogen peroxide. A similar decrease was observed in the DMPO-OH intensity in the presence of GIF (data not shown). In contrast to the effect of GIF, only a 10–20% decrease was observed in the presence of MT-I+II. The bimolecular rate constant for the reaction of hydroxyl radical with GIF, $k_{GIF/^{\cdot}OH}$, was estimated as 4.9×10^{13} M^{-1} s^{-1} by using the value $k_{DMPO/^{\cdot}OH} = 2.1 \times 10^{9}$ M^{-1} s^{-1} (17) and the ID_{50} value = 3.7 μM at a DMPO concentration of 83.6 mM.

To determine whether the difference in the hydroxyl radical-scavenging effect between GIF and MT-I+II is caused by the difference in metal supplementation, we assessed the scavenging activity of GIF or MT-I+II reconstituted with other metals in the hydroxyl radical generating system that utilizes photolysis. As shown in Table I, depletion of zinc from Cu,Zn-GIF reduced the scavenging activity for the hydroxyl radical, but replacement of cadmium by zinc in MT-I+II did not enhance the scavenging activity for hydroxyl radical. This suggests that the difference of metal in GIF and MT-I+II does not explain the difference in scavenging activity of the two proteins.

We examined the NO scavenging activity of GIF. Encapsulated PTIO in liposome reacts with NO and yields PTI stoichiometrically, of which the signals are distinguished by ESR. In this system, only untrapped NO, but not superoxide or various reducing agents outside of liposome, enters the liposomes and reacts with PTIO (Fig. 6*A*). Fig. 6*B* shows the ESR spectra of liposome PTIO before the addition of NOC-7, the NO-generating agent. The signal intensity of liposome PTIO decreased 15 min after the addition of NOC-7, with alternative increase in the signal intensity of liposome PTI. Fig. 6*B* also shows the ESR spectra of liposome PTI and residual liposome PTIO 15 min after the addition of NOC-7 to the mixture of liposome PTIO and GIF or MT-I+II. Neither GIF (0.95–7.60 μM) nor MT-I+II (0.84–6.74 μM) altered the signal intensity of liposome PTI (Fig. 6*B* and Table II), indicating that neither GIF nor MT-I+II trap NO generated from NOC-7.

We then determined whether GIF prevents the formation of 3-nitro-L-tyrosine by peroxynitrite. The tested compounds were human GIF, rat Cu-GIF, rat Cu,Zn-GIF, rabbit Cd,Zn-MT-I+II, rabbit Zn-MT-I+II, and glutathione. None of the tested compounds contained aromatic amino acids. As shown in Fig. 7, rat Cu-GIF (at 20–80 μM), rat Cu,Zn-GIF, and human GIF effectively inhibited the formation of 3-nitro-L-tyrosine by peroxynitrite. Cd,Zn-MT-I+II, Zn-MT-I+II, and glutathione at concentrations of 20–80 μM had weaker inhibitory activity on 3-nitro-L-tyrosine formation. These results indicate that GIF, like MT-I+II and glutathione, is an inhibitor of the tyrosine nitration by peroxynitrite, and the inhibitory effect of GIF on the tyrosine nitration does not depend on the metal content.

DISCUSSION

GIF is distributed throughout the soma and fine processes in astrocytes, but is restricted to axons and dendrites in a subset of neurons in the hippocampus and cerebral cortex. Despite the lack of a signal sequence in the GIF peptide, an extracellular:

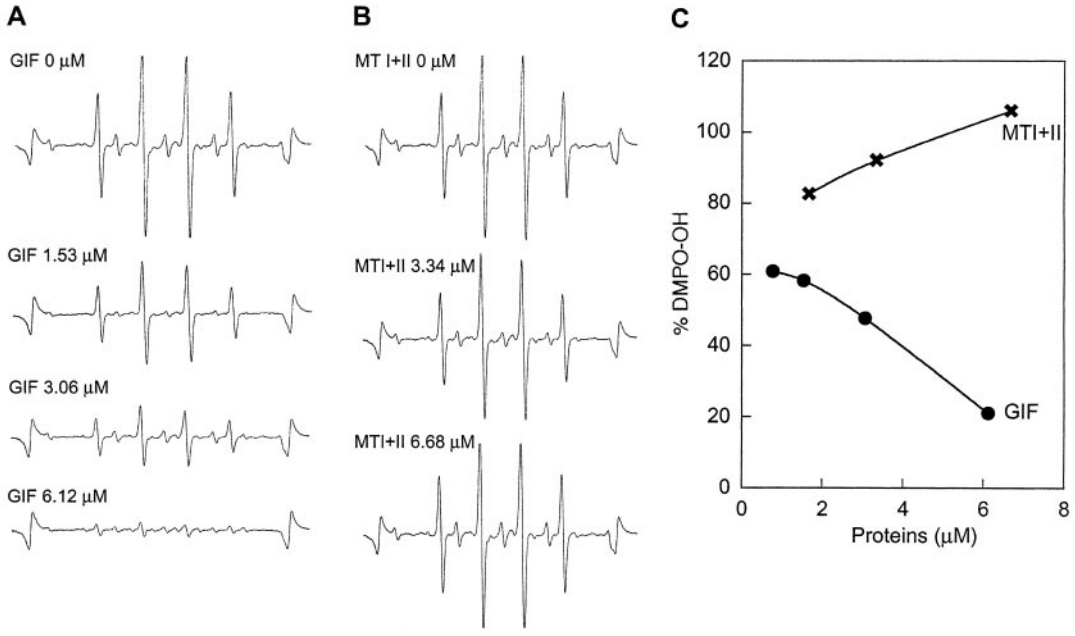

FIG. 5. **Human GIF scavenged hydroxyl radicals generated by a Fenton-type reaction.** *A* and *B*, ESR spectra of DMPO-OH in the presence of human GIF (*A*) or rabbit MT-I+II (*B*). *C*, the percentage intensities of DMPO-OH in the presence of various concentrations of GIF or MT-I+II. Hydroxyl radical, generated from the mixture of 0.34 mM H_2O_2 and 0.34 mM Fe^{2+} chelated with 0.34 mM DTPA, was trapped with 83.6 mM DMPO to produce a spin adduct (DMPO-OH). The signal intensities of DMPO-OH were evaluated by the relative peak height of DMPO-OH to the intensity of the Mn^{2+} signal. One hundred percent DMPO-OH was represented by the signal intensity of DMPO-OH obtained in the absence of the proteins.

TABLE I

Effect of metal content of GIF from rat brain or MT-I+II from rabbit liver on DMPO-OH formation by photolysis of hydrogen peroxide

Hydroxyl radical, generated from 2.3 mM H_2O_2 by photolysis, was trapped with 2.3 mM DMPO to produce a spin adduct (DMPO-OH). The signal intensities of DMPO-OH were evaluated by the relative peak height of DMPO-OH to the intensity of the Mn^{2+} signal. One hundred percent DMPO-OH was represented by the signal intensity of DMPO-OH obtained in the absence of the proteins.

Proteins	Formation of DMPO-OH
	%
No protein	100
Cu,Zn-GIF (2.5 μM)	58.5
Cu-GIF (2.5 μM)	89.9
Cd,Zn-MT-I+II (2 μM)	82.5
Zn-MT-I+II	
2 μM	83.9
4 μM	78.0
8 μM	78.8
16 μM	71.8

intracellular ratio of 1.29 for astrocytic GIF indicates that GIF is secreted from astrocytes by a regulated pathway (14). Exogenous GIF in the absence of brain extract from AD patients inhibited neurite extension from cortical neurons but did not inhibit neuronal survival in culture (Fig. 1). Instead, GIF maintained survival of neurons, as previously reported (5, 18). Because hyperoxia induces both neurite extension and neuronal death, it is reasonable to speculate that GIF protects cortical neurons from hyperoxia. Indeed, GIF prevented the induction of neuronal differentiation and neuronal death by high oxygen exposure (Fig. 2). Reduction of endogenous GIF in cortical neurons with an antisense ODN promoted neuronal death by high oxygen exposure (Fig. 3). Moreover, GIF effectively reduced ROS production, as detected using an indicator of intracellular ROS, in neurons induced by high oxygen exposure (Fig. 4), indicating that GIF protects cortical neurons from oxidative stress via scavenging not only extracellular but also intracellular ROS.

To determine which free radicals are targets of GIF, we used ROS and reactive nitrogen species generating systems coupled with ESR to evaluate the scavenging of superoxide, hydroxyl radicals, and NO by purified GIF. GIF scavenged neither superoxide generated in the hypoxanthine xanthine oxidase reaction nor NO generated from NOC-7, but did scavenge hydroxyl radicals generated in a Fenton-type reaction or by photolysis of hydrogen peroxide. Although the mechanism by which GIF but not MT-I+II acts as a scavenger for hydroxyl radicals is unclear, the scavenging activity was not the result of the metal-thiolate bonds of Cys-rich GIF, because MT-I+II, which has similar metal-thiolate coordination, did not show the scavenging effect for the hydroxyl radicals. It is not likely that the scavenging activity depends on the presence of copper in proteins (19). The hydroxyl radical scavenging activity of GIF was zinc-dependent but not copper-dependent (Table I). Even the replacement of cadmium in MT-I+II by zinc did not result in acquisition of scavenging activity for the hydroxyl radicals (Table I). In addition to the scavenging activity for hydroxyl radicals, GIF prevented nitration of tyrosine by peroxynitrite (Fig. 7). However, the scavenging effect for peroxynitrite may not be specific to GIF, because thiol groups of Cys in GIF, MT-I+II, and glutathione may responsible for the peroxynitrite scavenging.

Thus, extracellular GIF from astrocytes and/or intraneuronal GIF acts as a scavenger of hydroxyl radicals, and this may be responsible for the protective action of GIF against neurotoxicity and neurite sprouting induced by high oxygen exposure.

The interaction of MT-I or II with ROS or reactive nitrogen species has been reported previously; however, less attention has been paid to GIF (MT-III). Moreover, the ability of MT-I+II to protect against oxidative stress remains controversial. ESR spin-trapping studies indicate that MT-I+II have scavenging ability for superoxide (20, 21). However, in comparison with SOD, 300–30,000-fold higher concentrations of MT-I+II are needed for scavenging superoxide (21). There is also controversy about the hydroxyl radical scavenging abil-

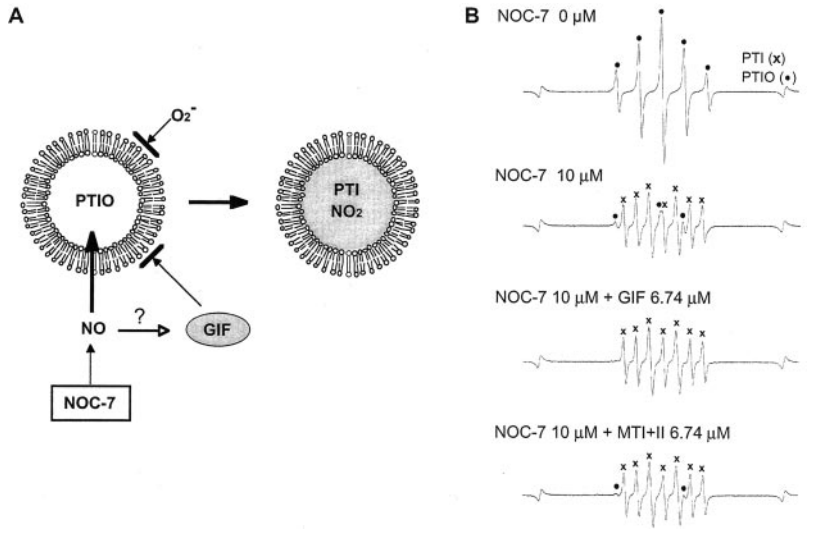

FIG. 6. **GIF did not scavenge NO generated by NOC-7.** *A*, schema of the reaction of liposome PTIO with NO. Only hydrophobic NO is accessible to the PTIO in the liposome vesicle. *B*, ESR spectra of liposome PTIO (×) before the addition of NOC-7 (*top*), and liposome PTI (●) and residual liposome PTIO (×) 15 min after the addition of NOC-7 to liposome PTIO alone (*middle top*) or with GIF (*middle bottom*) or MT-I+II (*bottom*). The reaction was initiated by the addition of NOC-7 (10 μM) to the mixture of protein solution and liposome PTIO (25 μM) suspension and then incubated for 15 min at 37 °C. PTI and unreacted PTIO were monitored by ESR spectroscopy. Spectra were recorded under the following conditions: microwave power, 5 milliwatts; modulation amplitude, 0.05 mT; time constant, 0.03; and sweep rate, 10 mT/min.

TABLE II
Effects of GIF from rat brain or MT-I+II from rabbit liver on liposome PTI formation by the addition of NOC-7 to liposome PTIO

The reaction was initiated by the addition of NOC-7 (10 μM) to the mixture of protein solution and liposome PTIO (25 μM) suspension, and incubated for 15 min at 37 °C. PTI and unreacted PTIO were monitored by ESR spectroscopy, and the relative signal intensities of PTI were calculated according to the previous report (12). One hundred percent formation of PTI was represented by the signal intensity of PTI obtained in the absence of the proteins.

Proteins	Formation of PTI
	%
No protein	100
GIF	
0.84 μM	96.5
1.68 μM	98.3
3.37 μM	103.2
6.74 μM	101.8
MT-I+II	
0.95 μM	94.5
1.90 μM	106.1
3.80 μM	101.0
7.60 μM	101.8

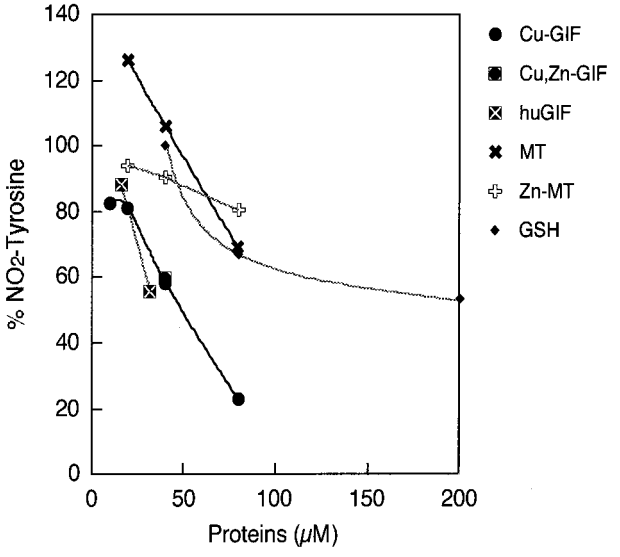

FIG. 7. **Human and rat GIF inhibited the formation of 3-nitro-L-tyrosine by peroxynitrite.** Peroxynitrite and L-tyrosine were mixed in PBS (pH 7.4) in the presence of various concentrations of the tested proteins: human GIF, rat Cu-GIF, rat Cu,Zn-GIF, rabbit Cd,Zn-MT-I+II, rabbit Zn-MT-I+II, and glutathione. The produced 3-nitro-L-tyrosine in the mixture was analyzed as indicated under "Experimental Procedures."

ity of MT-I and MT-II in spin-trapping studies. The scavenging activity of MT-I+II at high concentration (ID_{50} = 0.6 mM) for the hydroxyl radical was first reported by Thornalley and Vasak (20), and then further studied by Kumari *et al.* (22). However, Sakurai *et al*. (23), Suzuki *et al*. (24), and O'Brien and Salacinski (25) demonstrated that MT-I+II, especially Cu-MT, generated hydroxyl radicals in the presence of H_2O_2. Our studies indicated that MT-I+II at lower concentrations (1.67–6.68 μM) do not show scavenging activity for hydroxyl radicals. Specific scavengers for hydroxyl radicals are necessary for assessment of the scavenging activity of MT-I+II. In contrast to MT-I+II, GIF at a concentration of 6.8 μM competed for hydroxyl radicals with more than a 10^4-fold molar excess of DMPO, and the apparent bimolecular rate constant of $k_{\cdot OH/GIF} \approx 5 \times 10^{13}\ M^{-1}s^{-1}$ was extremely high, indicating that GIF has scavenging activity for hydroxyl radicals under conditions in which MT-I+II shows no scavenging activity for hydroxyl radicals.

It is controversial whether GIF is a scavenger for NO. Montoliu *et al.* (26) demonstrated NO quenching ability of GIF (MT-III) based on the loss of Cd(II) ions from GIF induced by the addition of an NO donor. Because they did not add EDTA to sample solutions to control the concentration of transition metals such as iron, sequestration of iron by GIF may occur under the condition of high concentrations of NO (27). It is likely that release of Cd(II) ions from GIF induced by the addition of NO may be caused by metal exchange from cadmium to iron in the GIF protein. Moreover, those authors did not compare the NO scavenging activity of GIF with that of a standard NO scavenger. We used liposome PTIO (a spin-trapping agent for NO) coupled with ESR to evaluate the scavenging ability of GIF outside the liposomes. In this system, only untrapped NO, but

not various proteins that reduce PTIO nonspecifically, enters liposomes, reacts with PTIO, and yields the mixture of PTI and unreacted PTIO, of which the signals are distinguished by ESR. The lack of alteration of the signal intensity of PTI inside liposomes by the addition of GIF or MT-I+II outside the liposomes (Fig. 6 and Table II) indicates that GIF does not compete for NO with PTIO, a NO scavenger.

Although the scavenging activity for hydroxyl radicals is observed specifically in GIF, other molecules containing thiol groups or aromatic amino acids also act as inhibitors of tyrosine nitration by peroxynitrite. Therefore, the protective effect of GIF on cultured cortical neurons against high oxygen exposure may be explained by the scavenging ability of GIF for hydroxyl radical rather than peroxynitrite.

The concentration of GIF required for significant protection against high oxygen toxicity (50–100 nM) is slightly higher than that required for inhibition of neurotrophic factors in AD brain extract ($EC_{50} \approx 14$–27 nM). However, the concentration of GIF required for neuroprotection is in the physiological range, because the average concentrations of GIF in adult rat brain or normal aged human brain determined by the two-site ELISA were 4–8 μg/g of brain (0.5–1 μM).

The results reported here indicate that GIF may play a role in reducing ROS via scavenging hydroxyl radicals in brain under physiological conditions. The reduction of GIF content in neurodegenerative disease (1–4) might result in the failure to eliminate ROS around/in neurons and may thus accelerate neuronal death.

Acknowledgment—We thank Dr. J. Shimizu for measuring the fluorescence-activated cell sorting spectra.

REFERENCES

1. Uchida, Y., Takio, K., Ihara, Y. & Tomonaga, M. (1991) *Neuron* **7,** 337–347
2. Uchida, Y. (1994) *Biol. Signals* **3,** 211–215
3. Arai, Y., Uchida, Y. & Takashima, S. (1997) *Pediat. Neurol.* **17,** 134–138
4. Kawashima, T., Doh-ura, K., Torisu, M., Uchida, Y., Furuta, A. & Iwaki, T. (2000) *Dement. Geriatr. Cogn. Disord.* **11,** 251–262
5. Erickson, J. C., Sewell, A. K., Jensen, L. T., Winge, D. R. & Palmiter, R. D. (1994) *Brain Res.* **649,** 297–304
6. Erickson, J. C., Masters, B. A., Kelly, E. J., Brinster, R. L. & Palmiter, R. D. (1995) *Neurochem. Int.* **27,** 35–41
7. Erickson, J. C., Hollopeter, G., Thomas, S. A., Froelick, G. J. & Palmiter, R. D. (1997) *J. Neurosci.* **17,** 1271–1281
8. Uchida, Y. (1999) *J. Neurochem.* **73,** 1945–1953
9. Uchida, Y. & Tomonaga, M. (1989) *Brain Res.* **481,** 190–193
10. Kobayashi, H., Uchida, Y., Ihara, Y., Nakajima, K., Kosaka, S., Miyatake, T. & Tsuji, S. (1993) *Mol. Brain Res.* **19,** 188–194
11. Mitsuta, K., Mizuno, Y., Kohno, M., Hiramatsu, M. & Mori, A. (1990) *Bull. Chem. Soc. Jpn.* **63,** 187–191
12. Akaike, T. & Maeda, H. (1996) *Methods Enzymol.* **268,** 211–221
13. Nakagawa, H., Sumiki, E., Takusagawa, M., Ikota, N., Matushima, Y. & Ozawa, T. (2000) *Chem. Pharm. Bull.* **48,** 261–265
14. Mignatti, P. & Rifkin, D. B. (1991) *J. Cell. Biochem.* **47,** 201–207
15. Kato, S., Mitusi, Y., Kitani, K. & Suzuki, T. (1997) *Biochem. Biophys. Res. Commun.* **241,** 347–351
16. Enokido, Y., Akaneya, Y., Niinobe, M., Mikoshiba, K. & Hatanaka, H. (1992) *Brain Res.* **599,** 261–271
17. Finkelstein, E., Rosen, G. M. & Rauckman, E. J. (1980) *J. Am. Chem. Soc.* **102,** 4994–4999
18. Amoureux, M. C., Wurch, T. & Pauwels, P. J. (1995) *Neurosci. Lett.* **201,** 61–64
19. Tamai, K. T., Gralla, E. B., Ellerby, L. M., Valentine, J. S. & Thiele, D. J. (1993) *Proc. Natl. Acad. Sci. U. S. A.* **90,** 8013–8017
20. Thornally, P. J. & Vasak, M. (1985) *Biochim. Biophys. Acta* **827,** 36–44
21. Hussain, S., Slikker, W., Jr. & Ali, S. (1996) *Neurochem. Int.* **29,** 145–152
22. Kumari, M. V. R., Hiramatsu, M. & Ebadi, M. (1998) *Free Radical Res.* **29,** 93–101
23. Sakurai, H., Satoh, H., Hatanaka, A., Sawada, T., Kawano, K., Hagino, T. & Nakajima, K. (1994) *Biochem. Biophys. Res. Commun.* **199,** 313–318
24. Suzuki, K. T., Rui, M., Ueda, J. & Ozawa, T. (1996) *Toxicol. Appl. Pharmacol.* **141,** 231–237
25. O'Brien, P. & Salacinski, H. J. (1998) *Arch. Toxicol.* **72,** 690–700
26. Montoliu, C., Monfort, P., Carrasco, J., Palacios, O., Capdevila, M., Hidalgo, J. & Felipo, V. (2000) *J. Neurochem.* **75,** 266–273
27. Kennedy, M. C., Gan, T., Antholine, W. E. & Petering, D. H. (1993) *Biochem. Biophys. Res. Commun.* **196,** 632–635